AIP | Applied Physics Letters

Plasma effects on the generation of reactive oxygen and nitrogen species in cancer cells in-vitro exposed by atmospheric pressure pulsed plasma jets

Sun Ja Kim and T. H. Chung

Citation: Applied Physics Letters **107**, 063702 (2015); doi: 10.1063/1.4928545
View online: http://dx.doi.org/10.1063/1.4928545
View Table of Contents: http://scitation.aip.org/content/aip/journal/apl/107/6?ver=pdfcov
Published by the AIP Publishing

Plasma effects on the generation of reactive oxygen and nitrogen species in cancer cells *in-vitro* exposed by atmospheric pressure pulsed plasma jets

Sun Ja Kim and T. H. Chung[a)]
Department of Physics, Dong-A University, Busan 604-714, South Korea

(Received 30 June 2015; accepted 2 August 2015; published online 11 August 2015)

Atmospheric pressure pulsed helium plasma jets are utilized for plasma-cell interactions. The effect of operating parameters such as applied voltage, pulse repetition frequency, and duty ratio on the generation of specific reactive oxygen and nitrogen species in gas and liquid phases and within cells is investigated. The apoptotic changes detected by terminal deoxynucleotidyl transferase (TdT)-mediated dUTP nick-end labeling assay in cells caused by plasma exposure are observed to correlate well with the levels of extracellular and intracellular reactive oxygen and nitrogen species. © *2015 AIP Publishing LLC*. [http://dx.doi.org/10.1063/1.4928545]

Various effects of atmospheric pressure plasma on living cells have been demonstrated.[1–3] Atmospheric pressure plasma jets (APPJs) enable the generation of a stable discharge that transports reactive species to a wanted site beyond the plasma-generating electrode.[4] The use of APPJs in cancer therapies is of particular interest because plasmas contain short-lived free radicals including reactive oxygen and nitrogen species (RONS) that can induce apoptosis in tumor cells.[5,6]

In the plasma treatment of living tissues, plasma species are delivered to the air-liquid interface and then undergo transportation and sometimes secondary generation of reactive radicals within the liquid medium before reaching cells and tissues.[4] Plasma-generated RONS depend on the plasma conditions controlled by many operating parameters. Thus, the investigation into the effects of operating parameters on plasma-cell interactions would be an important research topic for cancer therapeutic applications of atmospheric pressure plasmas.

Plasma-generated radical species are mainly reactive nitrogen species such as nitric oxide (NO) and nitrogen dioxide (NO_2) and reactive oxygen species (ROS) such as ozone (O_3), hydroxyl radicals (OH), superoxide anion (O_2^-), and singlet oxygen ($^1O_2$).[7] The interactions between the plasma and the liquid are of great interest and importance.[5] The hydroxyl-radical (OH) is one of the most active species generated in moist gas mixtures and is so reactive that it is thought to react with essentially any target.[1] The OH radicals are produced via diverse routes in gas phase, electron impact dissociation of H_2O molecules, the reactions of O (^1D) and N_2 (A) with H_2O molecules, the Penning and charge transfer reactions of H_2O molecules with excited species.[6,8,9] In liquid phase, they are produced in the pathway starting from superoxide anion and/or by dissociation of vibrationally excited water through collision with ground state water.[10]

Measuring the absolute density of OH species will improve the determination of treatment doses and allow for optimization of the plasma process for a specific application.[6] Moreover, of special interest is nitric oxide owing to its crucial role in both cell death and proliferation.[11] There is substantial literature on the role of NO and related compounds as a direct cancer therapy.[12,13] These studies provided evidence of an important tumor apoptotic intercellular signaling mechanism involving NO and $ONOO^-$.[12–14]

In plasma exposure to cells *in vitro*, the interaction of plasma species (excited neutral species and ions) with medium results in the generation of reactive species which can produce biologically important processes. Therefore, it is necessary to consider the interaction between a plasma jet and the liquid phase, particularly in the cell culture environment.[15] This paper examines the effect of the parameters such as applied voltage, pulse repetition frequency, and duty ratio of atmospheric pressure pulsed plasma jets on the RONS in gas and liquid phases and within cells. In order to examine plasma-induced chemistry effects, we used fluorescence probes (4, 5-diamino-fluorescein diacetate (DAF-2DA), 3′-(p-aminophenyl) fluorescein (APF), and Griess reagent to detect highly reactive species in living cells. The terminal deoxynucleotidyl transferase (TdT)-mediated dUTP nick-end labeling (TUNEL) technique was used for the detection and quantification of apoptosis after plasma treatment.

Figure 1(a) shows a photograph of the plasma plume and the schematic of the experimental setup of the jet source driven by a pulsed unipolar high voltage with a repetition rate of several tens of kHz (FT-Lab PDS 4000). The plasma jet consists of copper wire electrodes (2 mm diameter), polyetheretherketone (PEEK) plastic housing, and a pencil-shaped ring-grounded electrode (copper, 6 mm inner diameter and 16 mm outer diameter at the exit) covered with dielectric PEEK. A typical operating condition of the pulsed-dc plasma jet has applied voltage of 1.5 kV_{pp}, repetition frequency of 50 kHz, gas flow rate of 2 l/min, and duty ratio of 8%, unless otherwise stated. The optical emission spectra were recorded from the jet in the wavelength range of 200–900 nm using a fiber-optic spectrometer (Ocean Optics USB-2000). The plume temperature was measured using a fiber-optic temperature sensor (Luxtron, M601-DM&STF). A light-emitting diode (LED) light source (Ocean Optics, $\lambda = 310$ nm, FWHM 10 nm) was used to excite hydroxyterephthalic acid (HTA) in the cuvette, and the spectrum around $\lambda = 425$ nm was recorded through an optical fiber by a spectrometer.

[a)]Author to whom correspondence should be addressed. Electronic mail: thchung@dau.ac.kr

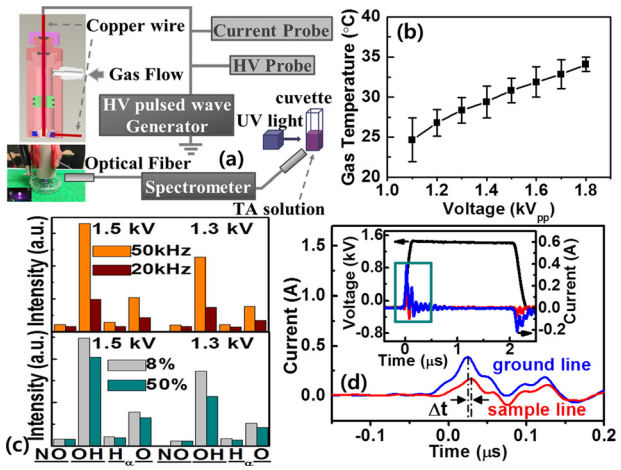

FIG. 1. (a) Schematic of experimental setup. (b) Gas temperature as functions of applied voltage and (c) variations of the emission intensities of NO, OH, O, and H_α as functions of applied voltage (1.3 and 1.5 kV_{pp}), repetition frequency (upper figure: 20 and 50 kHz), and duty ratio (bottom figure: 8% and 50%). (d) The waveforms of total current in the ring grounded electrode and sample electrode lines. The inset represents the waveforms of applied voltage and total current.

Figure 1(b) shows the measured gas temperature as a function of applied voltage. With an increase in the applied voltage, the plume temperature was increased. The temperature was less than 35 °C despite the high applied voltage. Figure 1(c) shows the variations of the emission intensities of NO, OH, O, and H_α via the optical spectra with the different operating parameters. It is observed that operation conditions under higher frequency and lower duty ratio results in the richness of these reactive species. Figure 1(d) represents the waveforms of total current in the ring grounded electrode and sample lines. The inset shows the waveforms of applied voltage and total current. The temporal delay (Δt) between current traces measured from ground and sample lines for the primary discharge offers information on the apparent plasma bullet propagation speed.[16] The drift velocity of plasma plume was estimated indirectly by the propagation speed of the luminous bullet by the time of flight method.[16,17] The plasma electron density is obtained by the ratio between the conduction current density and the product of electron charge and drift velocity.[16,17] The plasma plume current is estimated as a current measured in sample line. The cross-section of plume was estimated from the observation of the plasma plume by photographs. Using the average current value on the sample line and plasma plume diameter, the electron density was estimated as 1–6 $\times$ 10^{12} cm^{-3}. The electron density increased from 3.4 $\times$ 10^{12} to 5.41 $\times$ 10^{12} cm^{-3} with increasing applied voltage (1.5 kV_{pp} $\rightarrow$ 1.8 kV_{pp}) and increased from 1.12 $\times$ 10^{12} to 4.57 $\times$ 10^{12} cm^{-3} with decreasing duty ratio (35% $\rightarrow$ 8%).

RONS in the gas phase spread into the liquid phase and react with water to produce various biologically active reactive species. As a method of OH radical detection, we utilized the hydroxylation of TA, which is a typical photocatalytic reaction that specifically oxidizes TA; that is, the OH radical reacts with TA to form HTA. When the solution containing TA and HTA molecules is irradiated by UV light, the HTA molecules emit light.[8] Fluorescence intensity was observed to increase after reaction with plasma, indicating the increase in the OH radicals trapped by TA.

Figure 2 shows the fluorescence spectra of HTA as functions of operating conditions. Aqueous solution of TA was prepared by dissolving TA (Sigma) in distilled water containing NaOH (Wako). The initial concentrations of TA and NaOH were 3 mM and 10 mM, respectively, and the initial pH value was 8. The dish including liquids was irradiated with plasma (for 5 min), and samples of the liquids from the dish after plasma treatment were taken using a cuvette to observe the fluorescence after excitement by a light source. As the applied voltage (1.3 kV_{pp} $\rightarrow$ 1.7 kV_{pp}) and repetition frequency (20 kHz $\rightarrow$ 50 kHz) increased, the fluorescence intensity increased, indicating an increase in the OH radicals, as shown in Figs. 2(a) and 2(b). As the duty ratio decreased (30% $\rightarrow$ 8%), the intensity increased (Fig. 2(c)). These observations are in accordance with the intensity level of OH in optical spectra (Fig. 1(c)). It was observed that the plasma with gas mixtures containing 95% helium and 5% oxygen and 90% helium and 10% oxygen led to an increase of the fluorescence intensity (Fig. 2(d)). The OH density was observed to increase with both the applied voltage and pulse repetition frequency exhibiting a similar tendency to Ref. 18.

Reactive nitrogen species are also formed in the liquid phase. Nitrite concentration was determined using the Griess reagent (Molecular Probes). We used cell permeable reagents DAF-2 DA (Enzo Life Sciences) and APF (Sigma)). In liquids, nitric oxide is converted into nitrite and nitrate ions.[11] The Griess reaction can be used to analyze nitrite and can provide a good measure of the nitric oxide production.[11] Figure 3 shows the results of the nitric oxide quantitation assay performed on serum-free Hanks' balanced salt solution (HBSS, layer 3 mm) containing cells (or no cells). The dish including A549 cells (10^4 cells) was irradiated with plasma (0.5–3 min), and samples of the liquids from dish after plasma treatment were taken using a 96-well plate. The absorbance at 548 nm was measured using a spectrophotometer (Perkin-Elmer, CT) following incubation. In order to quantify the nitrite concentrations, a calibration curve was prepared using the standard sodium nitrite solutions (Molecular Probes). No significant difference is

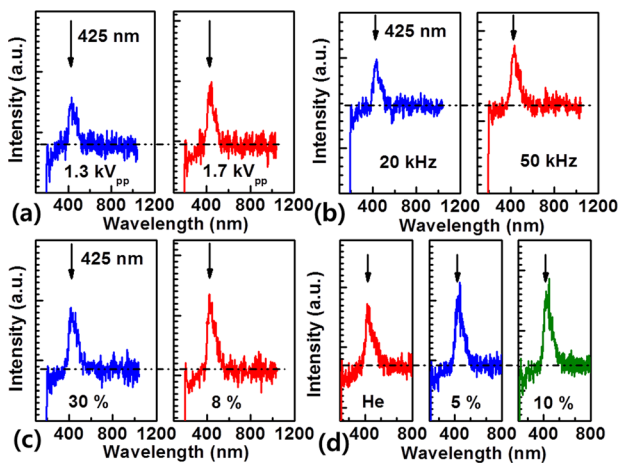

FIG. 2. Fluorescence spectra of aqueous TA solutions exposed to pulsed discharge as functions of (a) applied voltage (1.3 and 1.7 kV_{pp}), (b) repetition frequency (20 and 50 kHz), (c) duty ratio (8% and 30%), and (d) additive oxygen flow rate (0%, 5%, and 10%).

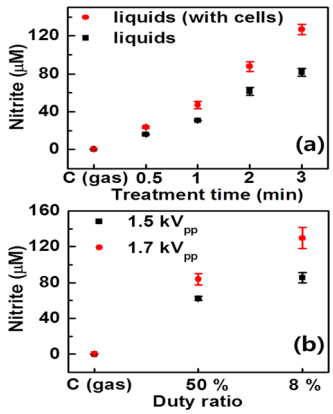

FIG. 3. Nitrite concentration as functions of (a) treatment time (0.5–3 min) in the presence and absence of cells, (b) applied voltage (1.5 and 1.7 kV_{pp}) and duty ratio (8% and 50%) (each point represents the mean ± SD of three replicates).

observed between the untreated control and gas-only exposure. On the other hand, the nitrite concentration increased after plasma exposure with increasing treatment time (Fig. 3(a)). It is observed that the concentration in the presence of cells is higher than that in the absence of cells. This suggests that plasma can influence NO production not only in the liquids but also in the cells despite the thick layer of buffer solution (serum-free). As the applied voltage increased (1.5 kV_{pp} → 1.7 kV_{pp}) and pulse duty ratio decreased (50% → 8%), the nitrite concentration increased, indicating the fact that the density of nitric oxide also can be controlled by plasma parameters of the discharge (Fig. 3(b)). It has been reported that the high production efficiency of reactive species is related to application of a voltage with a short pulse width.[19] The reason for this can be explained by two factors: larger electron density caused by a short pulse width and an increase of the active species mainly produced in primary streamer (N and O in our case). This may explain the reduction of nitrite concentration at higher duty ratio.

The intracellular generation of ROS after plasma treatment was detected by fluorescence microscopy using 2′, 7′-dichloro fluorescein diacetate (DCF-DA) (Molecular Probes), which diffuses into cells and is deacetylated by cellular esterases to non-fluorescent 2′, 7′-Dichlorodihydrofluorescein (DCFH). In the presence of ROS, DCFH is rapidly oxidized to highly fluorescent DCF.[20] A549 cells in dishes were pretreated with 10 μM DCF-DA for 5 min at 37 °C in the dark. Then, cells were exposed to plasma (and/or gas flow only) for 10 s on 9 points per dish and incubated for 5 min. Fluorescence-activated cells were detected and analyzed using a fluorescence microscopy. Figure 4 shows the fluorescence images of intracellular ROS production and bright field images. Figure 4(a) shows that plasma-treated cell populations containing high levels of DCF fluorescence were increased. However, the nonfluorescent H_2DCFDA becomes fluorescent in the presence of a wide variety of RONS including, but not limited to, peroxyl (ROO•) and hydroxyl (•OH) radicals and the peroxynitrite anion ($ONOO^-$). In contrast, APF has much more limited reactivity and higher resistance to light-induced oxidation; namely, fluorescein derivative is nonfluorescent until it reacts with the hydroxyl radical or peroxynitrite anion.[21] In order to examine more specific reactive species, we used APF (10 μM), and likewise, cells were loaded with the fluorescent cell-permeable NO-specific probe (DAF-2 DA; 10 μM). DAF-2 DA and APF were also performed by the same procedure that was used for DCF-DA assay. As shown in Fig. 4(b), the increase of NO-sensitive fluorophore was more specific and was observed in the plasma-treated area only (plume-cross section). Figure 4(c) shows intracellular OH generation after plasma treatment. It is observed that plasma induces a prompt cellular response (the track left by the plasma; the upper figures of Fig. 4(c)).

We examined plasma-induced cellular apoptotic death by using the TUNEL technique.[22] The extent of apoptosis was assessed with the APO-BrdU (deoxythymidine analog 5-bromo-2′-deoxyuridine 5′-triphosphate) TUNEL Assay kit (Molecular Probes). The cells (10^6 cells) were exposed for 5 min on a dish (with 3 mm thick layer of serum-free DMEM (Dulbecco's Modified Eagle's Medium)) with a distance of 10 mm between nozzle and cell surface. Cells were harvested by trypsinization 48 h after exposure to plasma and then fixed with 1% paraformaldehyde for 20 min in phosphate buffered saline (PBS). After fixation, the TUNEL assay was performed by following the manufacturer's instructions. The emitted green fluorescence from apoptotic cells was observed under fluorescence microscopy (Nikon TS100-F). Cell nuclei by propidium iodide staining were also observed with microscopy. As shown in Figs. 5(b) and 5(c), the ratio of TUNEL-positive cells increased after plasma treatment compared to that in gas-treated control cells (Fig. 5(a)). It is observed that the extent of apoptotic DNA fragmentation increased with increasing doses of plasma. The rate of apoptotic events increased from 4.7% to 37.5% with increasing applied voltage (1.4 kV_{pp} → 1.9 kV_{pp}).

Our previous studies[23,24] indicated that apoptosis was increased with increasing applied voltage and repetition

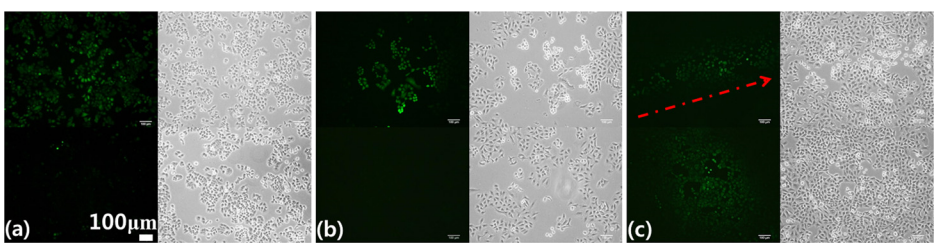

FIG. 4. Fluorescence images of intracellular ROS production and bright field images: by using (a) DCF-DA (upper row of figure: plasma-treated cells; bottom row of figure: gas-treated control cells), (b) DAF-2 DA (upper row of figure: plasma-treated cells; bottom row of figure: gas-treated control cells), and (c) APF (upper row of figure: the track left by the plasma; bottom row of figure: plasma-treated cells). The scale bar corresponds to 100 μm.

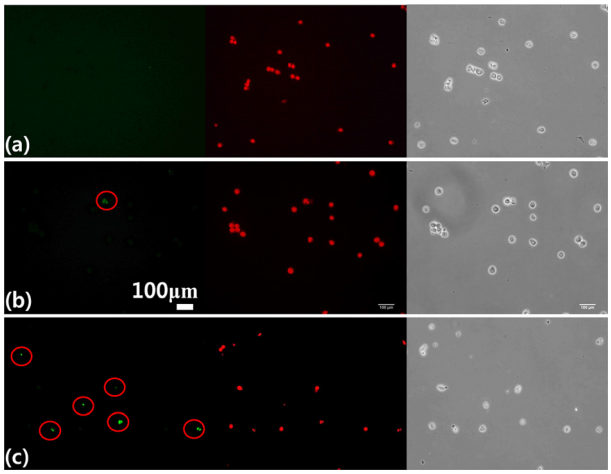

FIG. 5. TUNEL-positive (green) apoptotic cells (red circles), cell nuclei (red) by propidium iodide staining and bright field images: (a) gas-treated control cells, (b) plasma-treated (1.4 kV_{pp}) cells, and (c) plasma-treated (1.9 kV_{pp}) cells. The scale bar corresponds to 100 μm.

frequency and with decreasing duty ratio, and that the volume and luminosity of plasma bullet increased in the same manner. These observations agree well with the dependence of RONS measured in gas and liquid phases and within cells. These data suggest that the generation of intracellular RONS and the induction of apoptosis are the results of plasma's interaction with the extracellular medium and that the plasma effects depend on the concentration of active species in the medium (thus on the plasma dose).

In conclusion, the increase in applied voltage, pulse frequency, and decrease in duty ratio leads to an increase in the densities of OH and NO in gas and liquid phases and within a cell. Apoptosis rate correlates well with the levels of intracellular and extracellular RONS. Under the conditions of pulsed plasma experiments in this study, it can be concluded that the application of high voltage with 50 kHz frequency and duty ratio 8% results in the efficient production of reactive species for cancer cell treatment. These results could become potentially valuable information in utilizing atmospheric pressure plasma jets as a RONS-promoting cancer therapy.

This work was supported by the National Research Foundation of Korea (NRF) grant funded by the Korea Government (MSIP) (No. 2010-0027963).

[1]D. B. Graves, J. Phys. D: Appl. Phys. **45**, 263001 (2012).
[2]J. Y. Kim, S.-O. Kim, Y. Wei, and J. Li, Appl. Phys. Lett. **96**, 203701 (2010).
[3]S. J. Kim, T. H. Chung, S. H. Bae, and S. H. Leem, Appl. Phys. Lett. **97**, 023702 (2010).
[4]X. Lu, M. Laroussi, and V. Puech, Plasma Sources Sci. Technol. **21**, 034005 (2012).
[5]D. Mariotti, J. Patel, V. Svrcek, and P. Maguire, Plasma Processes Polym. **9**, 1074 (2012).
[6]X. Y. Liu, X. K. Pei, K. Ostrikov, X. P. Lu, and D. W. Liu, Phys. Plasmas **21**, 093513 (2014).
[7]J. Liebmann, J. Scherer, N. Bibinov, P. Rajasekaran, R. Kovacs, R. Gesche, P. Awakowicz, and V. Kolb-Bachofen, Nitric Oxide **24**, 8 (2011).
[8]S. Kanazawa, H. Kawano, S. Watanabe, T. Furuki, S. Akamine, R. Ichiki, T. Ohkubo, M. Kocik, and J. Mizeraczyk, Plasma Sources Sci. Technol. **20**, 034010 (2011).
[9]A. Komuro, R. Ono, and T. Oda, J. Phys. D: Appl. Phys. **46**, 175206 (2013).
[10]B. R. Locke and K. Y. Shih, Plasma Sources Sci. Technol. **20**, 034006 (2011).
[11]A. R. Gibson, H. O. McCarthy, A. A. Ali, D. O'Connell, and W. G. Graham, Plasma Processes Polym. **11**, 1142 (2014).
[12]D. B. Graves, Plasma Processes Polym. **11**, 1120 (2014).
[13]D. G. Hirst and T. Robson, Curr. Pharm. Des. **16**, 45 (2010).
[14]G. Bauer, Anticancer Res. **34**, 1467 (2014).
[15]K. Ninomiya, T. Ishijima, M. Imamura, T. Yamahara, H. Enomoto, K. Takahashi, Y. Tanaka, Y. Uesugi, and N. Shimizu, J. Phys. D: Appl. Phys. **46**, 425401 (2013).
[16]I. Topala and M. Nagatsu, Appl. Phys. Lett. **106**, 054105 (2015).
[17]K. Yambe, S. Taka, and K. Ogura, Phys. Plasmas **21**, 043511 (2014).
[18]X. Pei, S. Wu, Y. Xian, X. Lu, and Y. Pan, IEEE Trans. Plasma Sci. **42**, 1206 (2014).
[19]R. Ono, Y. Nakagawa, and T. Oda, J. Phys. D: Appl. Phys. **44**, 485201 (2011).
[20]T. M. Johnson, Z. X. Yu, V. J. Ferrans, R. A. Lowenstein, and T. Rinkel, Proc. Natl. Acad. Sci. U. S. A. **93**, 11848 (1996).
[21]K. Setsukinai, Y. Urano, K. Kakinuma, H. J. Majima, and T. Nagano, J. Biol. Chem. **278**, 3170 (2003).
[22]A. Nagoescu, P. Lorimier, F. Labat-Moleur, C. Drouet, C. Robert, C. Guillermet, C. Brambilla, and E. Brambilla, J. Histochem. Cytochem. **44**, 959 (1996).
[23]H. M. Joh, S. J. Kim, T. H. Chung, and S. H. Leem, Appl. Phys. Lett. **101**, 053703 (2012).
[24]S. J. Kim and T. H. Chung, IEEE Trans. Plasma Sci. **39**, 2280 (2011).